NUMERICAL AND EXPERIMENTAL STUDIES OF SELF-SYNCHRONIZATION AND SYNCHRONIZED CHAOS

by

M. de Sousa Vieira, P. Khoury, A. J. Lichtenberg,
M. A. Lieberman, W. Wonchoba, J. Gullicksen,
J. Y. Huang, R. Sherman, and M. Steinberg

Memorandum No. UCB/ERL M92/5

13 January 1992

NUMERICAL AND EXPERIMENTAL STUDIES OF SELF-SYNCHRONIZATION AND SYNCHRONIZED CHAOS

by

M. de Sousa Vieira, P. Khoury, A. J. Lichtenberg,
M. A. Lieberman, W. Wonchoba, J. Gullicksen,
J. Y. Huang, R. Sherman, and M. Steinberg

Memorandum No. UCB/ERL M92/5

13 January 1992

ELECTRONICS RESEARCH LABORATORY

College of Engineering
University of California, Berkeley
94720

NUMERICAL AND EXPERIMENTAL STUDIES OF SELF-SYNCHRONIZATION AND SYNCHRONIZED CHAOS

by

M. de Sousa Vieira, P. Khoury, A. J. Lichtenberg,
M. A. Lieberman, W. Wonchoba, J. Gullicksen,
J. Y. Huang, R. Sherman, and M. Steinberg

Memorandum No. UCB/ERL M92/5

13 January 1992

ELECTRONICS RESEARCH LABORATORY

College of Engineering
University of California, Berkeley
94720

NUMERICAL AND EXPERIMENTAL STUDIES OF SELF-SYNCHRONIZATION AND SYNCHRONIZED CHAOS

M. de Sousa Vieira, P. Khoury, A. J. Lichtenberg, M. A. Lieberman, W. Wonchoba

Department of Electrical Engineering and Computer Sciences
and the Electronics Research Laboratory
University of California
Berkeley CA 94720

and

J. Gullicksen, J. Y. Huang†, R. Sherman and M. Steinberg

Loral Aerospace
Western Development Laboratories
3200 Zanker Road, Bldg. 280, X21
San Jose, CA 95161-9041

ABSTRACT

We study self-synchronization of digital phase-locked loops (DPLL's) and the chaotic synchronization of DPLL's in a communication system which consists of three or more coupled DPLL's. Triangular wave signals, convenient for experiments, are employed. Numerical and experimental studies of two loops are in good agreement, giving bifurcation diagrams that show quasiperiodic, locked, and chaotic behavior. The approach to chaos does not show the full bifurcation sequence of sinusoidal signals. For studying synchronization to a chaotic signal the chaotic carrier is generated in a subsystem of two or more self-synchronized DPLL's, where one of the loops is stable and the other is unstable, i.e. their Liapunov exponents are negative and positive, respectively. The receiver consists of a stable loop. We verified numerically and experimentally that the receiver synchronizes with the transmitter if the stable loop in the transmitter and receiver are nearly identical and the synchronization degrades with noise and parameter variation. We studied the phase space where synchronization occurs, and quantify the deviation from synchronization using the concept of mutual information.

---

† Permanent address: *Electrical Engineering Department, San Jose State University, San Jose, CA 95192.*

I. INTRODUCTION

Analog and digital phase locked loops are devices used in a variety of communication applications such as modulation and demodulation, noise reduction and as synchronization devices to lock the phase of a receiver to that of a transmitter [1]. In a single DPLL the phase difference between transmitter and receiver is described by a circle map when the input is a sinusoidal signal with a constant amplitude and frequency [2,3]. Circle maps have been studied extensively in the past. They exhibit periodic cycles, quasiperiodic behavior and chaos[4]. For two coupled DPLL's we observed a more complicated behavior, but also characterized by periodicity, quasiperiodicity and chaos[5]. The coupled system can have more complicated bifurcation diagrams, and an important distinction exists between the dimensions of the attractors when one or both loops are chaotic, the attractor having higher dimensionality in the latter case[5].

The concept of synchronized chaos was introduced recently by Pecora and Carroll[6]. They showed how two near-identical systems linked by a chaotic signal can synchronize with each other. A potential application of this concept is to the problem of secure communications, the idea being to have two remote systems, linked by the same chaotic signals operate synchronously. This possibility was explored numerically in a system of coupled DPLL's[5]. Using two coupled loops, one stable and one unstable, as a transmitter of a chaotic signal, we showed that a third loop, nearly identical to the stable transmitter loop, can synchronize with that loop in the transmitter. The numerical study considered sinusoidal oscillators, which are more closely related to the well studied sine-circle map, but are more difficult to realize experimentally. In an introductory experimental study of synchronized chaos we used a simple experimental DPLL embodiment in which the oscillators have triangular output waveforms and the sampling is done at the zero-crossings. It was found experimentally that synchronization could be achieved, and this was confirmed numerically on analysis of a coupled system with similar characteristics[7].

In this paper we do more detailed numerical and experimental studies of self-synchronization of DPLL's and synchronization to a chaotic signal. The DPLL's considered here employ triangular wave forms sampling at the zero crossings. Studies were also made (not reported) sampling at the peak. In this case, the phase diagrams of the two coupled loops in the transmitter show different features; however for the chaotic synchronization studies we obtain qualitatively the same results. The paper is organized as follows: In section II we give a description of the system studied and present numerical results for the two coupled DPLL system. In section III we investigate the synchronization to a chaotic signal using these two coupled DPLL's as a transmitter and study the quantification of the synchronization using the concept of mutual information. In section IV we describe the experimental system and compare the numerical and experimental results. The last section gives our conclusions.

II. SYSTEM DESCRIPTION AND RESULTS FOR TWO COUPLED LOOPS

We first give a brief description of a single, first-order, nonuniformly sampling DPLL, whose block diagram is shown in Fig. 1. It consists of a sample-and-hold (SH) and a voltage controlled oscillator (VCO). During the operation, the SH takes a discrete sample $v(t_i)$ of the incoming signal at the sampling time t_i when the VCO signals it to do so. The sampled value is used to control the sampling frequency of the VCO according to a given function in such a way as to decrease the phase difference between the incoming signal and the oscillator output. As a result, for a range of parameters, there is a locked state when the oscillator frequency adjusts itself to the input frequency and locks to its phase, hence sampling always at the same point on the input signal. For other parameter regions multiperiodic orbits, quasiperiodicity and chaotic behavior may be observed.

It has been shown[3] that when the input signal is a sinusoid and the frequency of the VCO is linearly related to the sampled value $v(t_i)$ as

$$f' = f^o + b[v(t_i) + v^{off}], \tag{1}$$

then the phase difference between the signal and the VCO output is described by a circle map. In Eq. (1) f^o is the center frequency of the VCO, i.e., its frequency in the absence of applied signal, b is the loop gain, and v^{off} is an offset voltage that may be added to the input signal in order to bring it to the appropriate voltage range of operation in an experimental device.

Here we are concerned mainly with self-synchronized DPLL's where the input to one loop is given by a combination of the outputs of the other loops. Although explicit mapping equations can be constructed that describe the dynamics of such systems[8], we can numerically evolve the dynamics without finding such maps following the algorithms given in Refs. [3] and [5]. The transmitter system consisting of two coupled DPLL's is shown schematically in Fig. 2. In the experimental device studied the VCO outputs are voltages with triangular waveform, and the sample of the incoming signal is taken when the output voltage is zero with a positive slope. We use the convention that at this instant the phase (modulo 1) of the wave is zero. Thus we represent the output signal of the VCO's as $v(t) = A\Lambda(\phi(t))$ with

$$\Lambda(\phi(t)) = \begin{cases} 4\phi(t), & \text{if } 0 < \phi(t) \leq 1/4; \\ -4\phi(t) + 2, & \text{if } 1/4 < \phi(t) \leq 3/4; \\ 4\phi(t) - 4, & \text{if } 3/4 < \phi(t) \leq 1. \end{cases} \tag{2}$$

where $\phi(t) = ft$, with f the frequency, and $0 \leq t \leq 1/f$. In this coupled loop system each time that one of the triangular waves attains $\Lambda(\phi(t)) = 0$ with a positive slope the

oscillator sends a signal to its SH which then samples the VCO output of the other loop. The loop that samples switches its frequency to a new value given by

$$f_i' = f_i^o + b_i v(t_i) \tag{3}$$

For the two coupled DPLL's, for any time t, the system state is determined by four variables, the frequencies and the phases of the two loops. However, the system state changes only at the sampling instants. As a result, the dynamics lies in the union of two three-dimensional linear subspaces, which have $\phi_1 = 0 \pmod 1$ or $\phi_2 = 0 \pmod 1$. There are eight parameters in the coupled system. For each loop we have the amplitudes A_i's, the gains b_i's, the center frequencies f_i^o's and the offset voltages v_i^{off}'s. We can normalize the parameters in the following way. The equations that determine the dynamical evolution of the loops are

$$f_1' = f_1^o + b_1[A_2\Lambda(\phi_2) + v_1^{off}] \qquad (\phi_1 = 0), \tag{4a}$$

$$f_2' = f_2^o + b_2[A_1\Lambda(\phi_1) + v_2^{off}] \qquad (\phi_2 = 0). \tag{4b}$$

Dividing Eqs. (4) by $f_2^o + b_2 v_2^{off}$ we obtain

$$\overline{f}_1' = \overline{f}_1^o + B_1\Lambda(\phi_2), \tag{5a}$$

$$\overline{f}_2' = 1 + B_2\Lambda(\phi_1), \tag{5b}$$

where

$$\overline{f}_i' = \frac{f_i'}{f_2^o + b_2 v_2^{off}}, \quad \overline{f}_1^o = \frac{f_1^o + b_1 v_1^{off}}{f_2^o + b_2 v_2^{off}}, \quad B_i = \frac{b_i A_j}{f_2^o + b_2 v_2^{off}}. \tag{5c}$$

Thus there are three dimensionless fundamental parameters in the system, which are the two normalized gains B_1 and B_2 and the normalized center frequency $\overline{f}_1^o$ of one of the two loops, say loop 1. Since the frequencies of these discrete time systems are positively defined, we must have from Eqs. (5) that $B_1 < \overline{f}_1^o$ and $B_2 < 1$, since $\Lambda(\phi) \in [-1, 1]$.

We first analyze the locked state, i.e., when both loops synchronize to a common frequency $\overline{f}_s$. In this case $\phi_1(\phi_2 = 0) = -\phi_2(\phi_1 = 0) \equiv \Delta\phi$. From Eq. (5) we obtain

$$\overline{f}_s = \overline{f}_1^o + B_1\Lambda(-\Delta\phi), \tag{6a}$$

$$\overline{f}_s = 1 + B_2\Lambda(\Delta\phi). \tag{6b}$$

By noting that $\Lambda(\phi)$ is an odd function, we obtain from this system of equations:

$$\overline{f}_s = \frac{\overline{f}_1^o/B_1 + 1/B_2}{1/B_1 + 1/B_2}, \tag{7a}$$

$$\Lambda(\Delta\phi_s) = \frac{\overline{f}_1^o - 1}{B_1 + B_2}. \tag{7b}$$

Let us assume that $\overline{f}_1^o \geq 1$. In this case $\Delta\phi_s \in [0, 1/2]$. According to Eq. (7b) there are two possible values for the phase difference between the loops, that is, $\Delta\phi = \Delta\phi_s$ and $\Delta\phi = 1/2 - \Delta\phi_s$, since $\Lambda(\cdot)$ of these two angles are identical. We will show below that only one of these phase angles is stable. From Eq. (7b) one also sees that the synchronization is possible only if

$$B_1 + B_2 \geq |\overline{f}_1^o - 1|, \tag{8}$$

since $\Lambda(\cdot) \in [-1, 1]$.

As B_1 and/or B_2 increase bifurcations to higher period orbits are observed, which are followed by a chaotic regime. The parameter values where the first bifurcation occurs can be obtained analytically via a linear stability analysis. Suppose that we have a system of two coupled DPLL's in synchrony. In this case, the frequency of each loop is given by Eq. (7a), and the phase difference between them is determined by Eq. (7b). At $t = 0$, we perturb the frequency of VCO 1 to a new value given by $\overline{f}_s + \delta$. The evolution of the system after such a perturbation is shown schematically in Fig. 3. It is easy to show that at $t = t_2$ and $t = t_2'$ (where $\phi_2 = 0$) the phase difference between the loops is given respectively by

$$\phi_1(t_2) = (1 + \delta/\overline{f}_s)(1 - \Delta\phi_s), \tag{9}$$

and

$$\phi_1(t_2') = 1 - \Delta\phi_s + \frac{\delta}{\overline{f}_s}\left(1 - \frac{(B_1 + B_2)\Delta\phi_s(1 - \Delta\phi_s)\Lambda'(\Delta\phi_s)}{\overline{f}_s} + \frac{B_1 B_2 \Delta\phi_s(1 - \Delta\phi_s)^2 \Lambda'^2(\Delta\phi_s)}{\overline{f}_s^2}\right), \tag{10}$$

where we have neglected higher order terms in δ. The trace of the Jacobian matrix that transforms $\phi_1(t_2)$ into $\phi_1(t_2')$ is given by $T = \partial\phi_1(t_2')/\partial\phi_1(t_2)$. In this way we find

$$T = \frac{1}{1 - \Delta\phi_s} - \frac{(B_1 + B_2)\Lambda'(\Delta\phi_s)}{\overline{f}_s} + \frac{B_1 B_2 \Delta\phi_s(1 - \Delta\phi_s)\Lambda'^2(\Delta\phi_s)}{\overline{f}_s^2}. \tag{11}$$

In the above equations Λ' denotes the derivative of $\Lambda(\phi)$ with respect to ϕ. The synchronized state is stable if $|T| < 1$, and Eq. (8) is also satisfied. When $T = 0$ the system has its maximum stability and at $|T| = 1$ a bifurcation to a period 2 orbit appears. The first term in the right-hand side of Eq. (11) is greater than or equal 1 and the third term is positive. Thus, the second term must be negative in order to satisfy the condition that $|T|$ be smaller than 1 in the synchronized state. We have assumed that $\Delta\phi_s \in [0, 1/2]$. Therefore, the second term is negative only if $\Delta\phi_s \in [0, 1/4]$. This shows that the solution

$1/2 - \Delta\phi_s$, which satisfies Eq. (7b) is unstable. If we start with the assumption that $\overline{f}_1^o < 1$, then we will reach similar conclusions, i.e., there is only one stable solution for the phase difference between loops, which now is situated in the interval $\Delta\phi_s \in [3/4, 1]$. If the center frequencies of the loops are identical, that is, $\overline{f}_1^o = 1$, then the above expression for the bifurcation point simplifies to $B_1 + B_2 = 1/2$, since $\overline{f}_s = 1$ and $\Delta\phi_s = 0$. The maximum stability is attained at $B_1 + B_2 = 1/4$.

We show in Fig. 4 a typical bifurcation diagram of ϕ_1 versus B_2 at the surface of section $\phi_2 = 0$ for $B_1 = 0.2$ and $\overline{f}_1^o = 1$. In all the numerical simulations associated with the coupled loops we use the following initial conditions $\phi_1 = \phi_2 = \phi_3 = 0$, $\overline{f}_1 = 1.0$, and $\overline{f}_2 = 1.1$. A transient of typically 1000 iterations is neglected. The route to chaos in this system is not via period doubling bifurcations, as in the case studied in [5]. Here the sequence is truncated beyond the period four cycle and a complex entrance into chaos is observed.

The complete phase diagram of the coupled loop system is situated in a tri-dimensional space, since we have three fundamental parameters. Here we study some particular planes of the phase diagram to find the regions where chaotic motion is present. In the first case we take $B_1 = 0$. This corresponds to the case in which the coupling between loops is only in one direction. That is, the input of loop 2 is a triangular wave with constant frequency $\overline{f}_1^o$. Similarly to what was done in Ref. [3], we can easily derive that the phase difference between loops 1 and 2 at the sampling instant of loop 2 is given by

$$\phi_1' = \phi_1 + \frac{\overline{f}_1^o}{1 + B_2\Lambda(\phi_1)}, \tag{12}$$

This is a one-dimensional nonlinear map which shares some properties with the sine circle maps, but because of the discontinuity in the $\Lambda(\phi)$ derivative this map has a phase diagram that is topologically different from the diagram of the circle map. In Fig. 5 we show the phase diagram of the map governed by Eq. (12). The black regions have positive Liapunov exponent λ. The Liapunov exponent measures the rate of the exponential separation between two neighboring trajectories, and it is defined as[9]

$$\lambda = \frac{1}{N-1} \lim_{N\to\infty} \sum_{n=1}^{N} \log |(d\phi_1'/d\phi_1)^n|, \tag{13}$$

where the superscript n denotes the iteration index. If a system has at least one positive Liapunov exponent in a given region of the parameter space, then the system is chaotic in that region. We considered λ positive in the calculations when $\lambda > 10^{-3}$ for $N = 30,000$. In the region where chaotic motion can appear the map is noninvertible. The border of invertibility of Eq. (12) is shown in Fig. 5 by a dashed line and is determined by $\overline{f}_1^o = (1 - B_2)^2/(4B_2)$. Thus, below the dashed line only periodic or quasiperiodic motion

is allowed. In the nonchaotic region we observe the existence of tongues of stability similar to the Arnold tongues. The tongues are characterized by the winding numbers W defined by

$$W = \lim_{t\to\infty} \frac{\phi_1(t) - \phi_1(0)}{\phi_2(t) - \phi_2(0)} \tag{14}$$

The largest tongues are labelled in Fig. 5 by the corresponding winding numbers. One can see that this phase diagram is not topologically identical to the phase diagram of a sine circle map. For instance, at $\overline{f}_1^o = 1$ a sine-circle map would display a sequence of period doubling bifurcations, which is not observed here. The bifurcation sequence in our map is truncated at the 2-cycle because of the discontinuity in the derivative of $\Lambda(\cdot)$ at the maximum.

We study two simplified cases of the fully coupled system. First we study the plane $B \equiv B_1 = B_2$, where the coupling in both directions has the same strength. The calculation of the Liapunov exponents following directly the dynamics of the system is not straightforward, because the coupled loop is described by discontinuous mapping equations[8]. To characterize regions of chaotic motion, we used the algorithm given in Ref. [10] for the study of Liapunov exponent associated with time series. We plot in Fig. 6a for the plane B vs. $\overline{f}_1^o$, the regions where the motion is non chaotic as the white part. The shaded part indicates regions where the Liapunov exponent is positive. We consider the exponent positive when its absolute value is greater than 10^{-2} for a time series of 1000 points. The largest "Arnold tongues" are labelled by the corresponding winding numbers. We do not observe any topological difference between this diagram and the one shown in Fig. 5. We expect that quasiperiodic behavior, in analogy with the map governed by Eq. (12), will be found in regions where B is small. The dots there are probably due to the fact that the lenght of the time series used is short for the algorithm to distinguish quasiperiodic from chaotic behavior at those parameter values. For large B the motion in most of the shaded part is seen to be chaotic. Now we consider $\overline{f}_1^o = 1$ and plot in Fig. 6b (shaded) the regions in the B_2 vs. B_1 plane where the motion is chaotic. The winding numbers of some periodic regions are specified in the figure.

III. CHAOTIC SYNCHRONIZATION AND MUTUAL INFORMATION

We consider in this section the synchronization to a chaotic signal produced by the coupled DPLL's. The synchronization is obtained by transmitting a variable of the chaotic driving system (the transmitter) to the response system (the receiver), which is nearly identical to a subsystem of the transmitter. The schematic of the system is shown in Fig. 2. We observe numerically that loops 1 and 3 synchronize with each other in certain regions of the parameter space, even when the transmitter is chaotic. The necessary condition for

this to happen is that the Liapunov exponents associated with loops 1 and 3 be negative. Due to the presence of more than one basin of attraction, or to other factors, loops 1 and 3 do not always synchronize, as we discuss below.

We show in Fig. 7a the regions (white) where synchronization is observed between loops 1 and 3 for $B_1 = B_2 = B_3 \equiv B$ in the plane B vs. $\overline{f}_1^o = \overline{f}_3^o$. The third loop is started with the initial conditions $\phi_3 = 0$ and $\overline{f}_3 = 1.2$. When Fig. 7a is compared with Fig. 6a, one sees that synchronization may be observed when the transmitter is chaotic and also that there are regions where the transmitter has a periodic behavior and synchronization between loops 1 and 3 is not found. Note that the transmitter in our system, consisting of two self-synchronized coupled DPLL's, is intrinsically different from the receiver, where the coupling is only in one direction. We observe that this lack of symmetry between the transmitter and receiver causes the nonsynchronization between loops 1 and 3 in the regions where periodic behavior exists in the transmitter, as well as in the receiver. This is seen, for instance, when B is small and $\overline{f}_1^o = \overline{f}_3^o$ is close to 3 or 4. We checked several sets of initial conditions and the synchronization of loops 1 and 3 was never obtained in these periodic regions. In Fig. 7b we show the region (white) of synchronization between loops 1 and 3 for the plane B_2 vs. $B_1 = B_3$ and $\overline{f}_1^o = \overline{f}_3^o = 1$. We also observe chaotic synchronization for $B_1 \lesssim 0.5$ and $B_2 \gtrsim 0.5$. Again nonsynchronization between loops 1 and 3 in regions where the transmitter is periodic is found. This occurs, for instance, for the period 4 region with $B_2 < B_1$. The nonsynchronization is again due to the lack of symmetry between the first and the third loop.

It has been noted that when synchronization between the master and slave systems occurs, then the dimensionality of the system as a whole is smaller than in the case the synchronization is not observed[11]. We confirm this fact in our system by calculating the correlation dimension of the chaotic attractors associated with chaotic synchronization and a fully chaotic system where synchronization cannot be observed. The correlation dimension represents a lower bound to the number of independent variables necessary to describe or model the underlying dynamics of the attractor. In general, for chaotic attractors, if this positive defined dimension is a fractional number, then the bound is the next integer[12]. The chaotic attractors obtained by plotting ϕ_3 vs. $\overline{f}_3'$ at $\phi_2 = 0$ are shown in Fig. 8. The first case, Fig. 8a, corresponds to the strange attractor obtained for $B_1 = B_3 = 0.2$, $B_2 = 0.6$ and $\overline{f}_1^o = \overline{f}_3^o = 1$, where loops 1 and 3 synchronize. In Fig. 8b the attractor for $B_1 = B_2 = B_3 = 0.6$ and $\overline{f}_1^o = \overline{f}_3^o = 1$ corresponds to nonsynchronization between receiver and transmitter, due to the fact that all loops have positive Liapunov exponents. In the second case, the attractor explores more regions of the phase space. We calculated the correlation dimension d_c for the attractors shown in Fig. 8 using the algorithm given in Ref. 12. We find for the synchronized case (Fig. 8a) $d_c \approx 1.3$. For the attractor shown in Fig. 8b we found $d_c \approx 2.2$. The data used in the calculation are the

phases of the third loop when $\phi_2 = 0$. Thus the underlying dynamics for the communication system for these parameter sets are described by at least two and three variables for the cases where synchronization and nonsynchronization is observed, respectively.

In a practical situation, it would not be possible to make the parameters of loops 1 and 3 completely identical. However, we observe that even in the case that the stable loops in the transmitter and receiver are not identical, the synchronization persists, but with some error between the dynamical values of the master and slave system. We observed in our simulations that the loss of correlation between the transmitter and receiver strongly depends on the parameter that is being varied. In our communication system we found that the degree of correlation is much more sensitive to a given percentage change in the center frequencies, than in the gains. This is illustrated in Fig. 9, where we show the output voltage of loop 3 versus the corresponding quantity for loop 1 for two cases: (a) when the gains B_1 and B_3 are slightly different, and (b) when the center frequencies $\overline{f}_1^o$ and $\overline{f}_3^o$ have the same absolute variation, that is, $|B_1 - B_3| = |\overline{f}_1^o - \overline{f}_3^o|$. Observe that in the second case the correlation between the two loops is smaller that in the first case, even with the same absolute deviations in the parameters, which represents a much smaller relative change in the center frequencies.

The degree of correlation between transmitter and receiver can be quantitatively characterized by using the concept of mutual information. It is well known that the mutual information is a better quantity to measure dependence than the correlation function, which only measures the linear dependence. We briefly review the basic definition of mutual information[13]. Consider a dynamical system that is described by the discrete variable X_1 and that this system has relaxed to an attractor. One starts by dividing the phase space of X_1 into N boxes. Denote by $p(i_1)$ the probability that a measurement of the system will find the variable X_1 in the ith box. Do the same for X_2. If two systems are measured simultaneously, then the relevant probability distributions are $p(i_1)$, $p(i_2)$, and the joint probability distribution $p(i_1, i_2)$. The mutual information is defined as

$$I(X_1, X_2) = \sum_{i_1, i_2} p(i_1, i_2) \log_2 \left[\frac{p(i_1, i_2)}{p(i_1) p(i_2)} \right], \tag{15}$$

where the sum extends over all elements of the joint partition for which $p(i_1)$ and $p(i_2)$ are both nonzero. The mutual information gives the amount of information gained, in bits, about one system from a measurement of the other. It is a dynamical invariant, i.e., it does not depend on the system of coordinates used. When the number of cells of the phase space partition N is increased, the resolution of measurement is also increased, as well as the information about the state of the system. Consequently, the mutual information will depend on N. If X_1 and X_2 are independent, then $p(i_1, i_2) = p(i_1)p(i_2)$ and $I(X_1, X_2) = 0$. Mutual information was recently used in the context of chaotic synchronization[11]. It was

shown that the mutual information is large when two subsystems are operating in a regime of chaotic synchronization and rapidly decreases to a small value when all subsystems are operating in a chaotic regime.

We calculated the mutual information for the three loop system shown in Fig. 2. We analyzed two cases described below, using 20,000 points in the computation after the transient died. We divided the interval [-1,1] (range of the voltage signal) into 50 boxes. The data used in the calculation are the values of the voltage of the signals of loops 1 and 3 when loop 2 samples. If we use the phase as the variable studied, instead of the voltage, the results obtained are very similar to the ones that we will show. We take $B_1 = 0.2$, $B_2 = 0.6$, $\overline{f}_1^o = \overline{f}_3^o = 1$ and in the first case we vary B_3. We show in Fig. 10a I vs. B_3. The mutual information between loops 1 and 3 has a peak at $B_3 = B_1$ where the receiver and transmitter are completely synchronized. Also, it is seen that the mutual information is asymmetric with respect to the maximum. It decreases quite slowly, especially for $B_3 > B_1$ and at B_3 close to 0 or 1, I is very small and the loops are practically uncorrelated. In the other case, shown in Fig. 10b, we vary $\overline{f}_3^o$. Here we also observe a peak when $\overline{f}_3^o = \overline{f}_1^o$, and also I is asymmetric with respect to the maximum. We see, however, that the mutual information decreases faster when compared with the case shown in Fig. 10a. This implies that if for security reasons one needs a communication system that is very sensitive to variations in the parameters, then the center frequency of the transmitter is an important quantity to be used as a key.

IV. EXPERIMENTAL RESULTS

We have experimentally investigated the transmitter system consisting of two coupled loops, and the transmitter-receiver combination. The experimental circuit for a single DPLL, shown in Fig. 11, is composed of two main parts: (1) the sampler and associated support circuitry and (2) the VCO and associated circuitry. Although more than one device has been used, we shall describe the parameters of one of them, as a specific example. For the sampler a National Semiconductor LF398 monolithic sample and hold (SH) circuit is used. A 0.001 μF polystyrene capacitor is used for its low dielectric loss properties as the hold capacitor. The sample time is set by a 74LS123 retriggerable monostable multivibrator. The pulse width of the multivibrator is set with $R_{ext} = 20\ k\Omega$ and $C_{ext} =$ 680 pF which gives a predicted pulse duration of about 6.7 μs[14] and a measured pulse duration of about 6.0 μs. The maximum frequency of the input signal is about 2.0 kHz. Therefore, our sampling duration is about 1.2% of the signal period in the worst case and less than 1% on average. Hence, our sampling error should be much less than 1%.

For the VCO a National Semiconductor LM566C voltage controlled oscillator (VCO) integrated circuit is used. The frequency of the VCO is given approximately by the for-

mula[15]

$$f = \frac{2.4(V^+ - v_5)}{R_1 C_1 V^+}, \tag{16}$$

where $V^+ = 5V$, v_5 is the control voltage input (the voltage on pin 5 minus the voltage on pin 1 of the integrated circuit), $R_1 = 10$ kΩ and $C_1 = 0.022$ μF. Due to the relatively loose tolerances of R_1 and C_1 and the temperature dependence of these components, Eq. (16) is useful primarily for design purposes. The output of the VCO has an amplitude of 0.9 V and a D.C. offset of -0.9 V. To use this VCO in a DPLL it is necessary to add a DC offset voltage either to the input signal to the sampler or to the output signal of the sampler so that the input signal to the VCO will be in the proper voltage range. The operational amplifier circuit shown in Fig. 11 is used to adjust the offset voltage. A hard limiter LM311 with a reference of -0.9 V was included at the triangle wave output of the VCO to cause sampling at the zero crossing, as opposed to sampling at the peak, as in the case of the circuit studied in Ref. 3.

In the experimental systems we studied both pairs of self-synchronized DPLL's (the transmitter) and synchronization to a chaotic signal with three DPLL's as shown schematically in Fig. 2. The measurements of self-synchronization involved varying parameters over wide ranges to obtain bifurcation diagrams, surface of section plots of attractors, etc. This required automated systems to perform the scans, so modifying the basic circuitry.

Two digital-to-analog (DAC) circuits placed between the SH and the VCO comprise the heart of the automation. One DAC adjusts the gain parameter while the other adjusts the center frequency. Hence the amplifier that would come directly after the SH circuit, is now replaced with a DAC and a series of amplifiers. The voltage from the sample and hold feeds into the DAC where it is amplified by an amount proportional to the digital input. This DAC controls the frequency span parameter. The last amplifier in the chain receives this amplified signal and offsets it with a voltage controlled by the second DAC. This DAC controls the center frequency parameter. The computer control allows the parameters to be scanned. The voltage input to the SH falls in a fixed range which depends on the VCO feeding the signal but not on the frequency of the input signal. Some of the external support circuitry surrounding the PLL enables the computer to send known test signals as input to each VCO. The computer applies a voltage at the peak of the input range and measures the associated frequency, then it applies the lowest possible voltage in the range and measures that frequency. From these two measurements the computer can determine the current values of the span and center frequencies parameters. Once the current values are known the computer can adjust the circuit to values that fit the desired parameters.

Automation allows efficient measurement of the variables. The measurement capability is implemented with a 1 MHz clock, a number of counters, and several data latches. These enable the computer to detect which loop sampled and the time between successive

samples. The counters are always fed with a 1 MHz signal and thus provide a clock whose resolution is 1 μs. The same signal that triggers the sample and hold within the PLL goes to one of two latches and triggers the storage of the current value of the counters. The computer can then read the value stored in the latch and reset the latch reading it to take a new measurement at its own speed. A separate latch is needed to store the sampling time for each loop because if each loop samples at approximately the same time the computer cannot read the two pieces of data fast enough and data would be lost. Such a situation occurs when the two loops are in synchronization.

The experimental results of the coupled two loop system are shown in Figs. 12 and 13. In Fig. 12 the bifurcation diagram obtained experimentally in the coupled loops has the parameters values used in the numerical results shown in Fig. 4. In the figure representing the experimental results there is a gray scale where the darker regions represent the points with more frequent visits. Comparing Fig. 12 with Fig. 4 we observe a good agreement between the numerical results and the experiment, including the qualitative representation of the invariant density distribution in the chaotic regime. In addition, the experiment shows points off the attractor induced by noise, with the light gray indicating infrequent visits to those sites (in fact, single visits). In Fig. 13 we show the experimentally determined attractor in the plane ϕ_1 versus $\overline{f}_1'$ for the parameter values used numerically to make Fig. 8a. Again we observe a good agreement between theory and experiment, with the thickening of the attractor the result of experimental noise.

We also experimentally studied the synchronization to a chaotic signal in our communication system shown in Fig. 2. As predicted in our numerical simulations, we observe in the experimental device a parameter region where synchronization in the chaotic regime is obtained. We illustrate this by showing in Fig. 14a the output voltage of loop 3 versus the corresponding quantity for loop 1. Since in the experimental system noise is unavoidable the synchronization between the two loops is not perfect. The normalized parameters for this chaotic synchronized case are approximately $B_1 = 0.720$, $B_2 = 0.694$, $B_3 = 0.718$, $\overline{f}_1^o = 1.154$ and $\overline{f}_3^o = 1.152$.

By varying the parameters of loop 3 in relation to loop 1 we study experimentally the loss of synchronization between the transmitter and receiver. This is shown in Fig. 14b, where now $\overline{f}_3^o = 1.110$.

V. CONCLUSIONS AND DISCUSSIONS

We have studied the self-synchronization of two DPLL's mutually connected, and the synchronization to a chaotic signal in a system of coupled DPLL's. For the latter case the transmitter consists of two self-synchronized DPLL's, 1 and 2, and the receiver consists of a third loop, 3. The locked state for the two coupled loops was analyzed analytically

and in the phase diagram we identified the regions of chaotic and non chaotic motion. Tongues of periodic behavior were characterized by the corresponding winding numbers. We studied the fractal dimension of the attractor in the output of the receiver and verified that it has a larger dimension when the loops are chaotic and nonsynchronized, than when we have chaotic synchronization. The two-loop self-synchronized system was also studied experimentally using a novel computer control system to rapidly acquire data and present it in a manner to compare easily to the computations. The results gave good agreement between experimental and numerical results, indicating that the numerical results can be relied upon for first order understanding of the experimental devices. The effects of noise in the experiment were also clearly delineated.

We also studied numerically the region of synchronization between loops 1 and 3 in some planes of the parameter space where the phase diagram was investigated. We used the concept of mutual information to quantify the degree of correlation between transmitter and receiver. We verified that deviations in the center frequencies of the stable loops in the transmitter and receiver have a larger effect on the loss of synchronization, than deviations in the gains of the loops. In a parameter regime in which loop 2 is chaotic and loops 1 and 3 are stable, we experimentally studied the synchronization between loops 1 and 3, and compared the results with the numerical results. We found that synchronization was not significantly degraded by noise, and that detuning of the parameters degraded the synchronization approximately the same as observed numerically.

We tested the idea of chaotic synchronization in a more complex system where the transmitter consists of a ring of three loops, 1, 2, 3 and the receiver of two loops, 4 and 5. Thus, for the receiver we have four control parameters governing its behavior, i.e., two center frequencies and two gains. The output of loop 3 feeds loop 2 and 4. We verified that only in the case that loop 1 and loop 2 are completely identical to loops 4 and 5, respectively, that perfect synchronization between loops 2 and 5 is achieved, as well as between loops 1 and 4. If one of the loops 4 or 5 is not identical to its respective loop in the transmitter, then the synchronization between transmitter and receiver is affected.

More complex configurations could be imagined. However we argue that no chaotic loop should exist in the receiver. If there is a chaotic loop in the receiver, then due to the sensitivity to the initial conditions we do not expect synchronization between the receiver and the transmitter, even if there is parameter matching. In this case, an infinitely small difference in the initial conditions between the transmitter and the receiver will increase exponentially in time. On the other hand, the existence of several chaotic loops in the transmitter may be a desirable configuration for secure communication applications, since this could make the transmitted signal look more chaotic, having a higher dimensionality. Our preliminary results show that the addition of another chaotic loop in the transmitter increases the correlation dimension of the output signal of the transmitter by roughly one.

Our results indicate the possible usefulness of synchronization of chaotic signals for secure communications[7]. Various signal recovery schemes are available to extract the synchronized information from a noisy signal. In fact, one mechanism for lowering the probability of detection is to embed the signal in noise before it is sent. In order to be used in a communication system the signal must be modulated, and the techniques for modulation are currently under investigation. An important part of the numerical and experimental program is to understand the effect of noise on the accuracy of recovering a modulated signal, which is a current direction of our research.

ACKNOWLEDGMENTS

This work was partially supported by DARPA Grant W-SO-242614-T-12/91.

REFERENCES

[1] R. E. Best [1984] *Phase Locked Loops* (McGraw-Hill Books Company; W. C. Lindsey and C. M. Chie [1981] "A Survey of Digital Phase-Locked Loops", *Proc. IEEE* **69**, 410-431 .

[2] S. Gil and S. C. Gupta [1972] "First-Order Discrete Phase-Locked Loop With Applications to Demodulation of Angle-Modulated Carrier", *IEEE Trans. Commun.* **20**, 454-462; S. Gil and S. C. Gupta [1972] "On Higher Order Discrete Phase-Locked Loops" *IEEE Trans. Aerosp. Electron. Syst.* **8**, 615-623.

[3] G. M. Bernstein, M. A. Lieberman and A. J. Lichtenberg [1989] "Nonlinear Dynamics of a Digital Phase Locked Loop", *IEEE Trans. Commun.* **37**, 1062-1070; G. M. Bernstein and M. A. Lieberman [1990] "Secure random number generation using chaotic circuits" *IEEE Trans. Circuits Systems* **37**, 1157; G. M. Bernstein, *Nonlinear Oscillations, Synchronization and Chaos*, PhD thesis, University of California, Berkeley, 1988.

[4] S. J. Shenker [1982] "Scaling Behavior in a Map of Circle onto Itself: Empirical Results", *Physica* (Utrecht) **5D**, 405-411; M. J. Feigenbaum, L. P. Kadanoff, and S. J. Shenker [1982] "Quasiperiodicity in Dissipative Systems: A Renormalization Group Analysis", *Physica* (Utrecht) **5D**, 370-386; D. Rand, S. Ostlund, J. Sethna, and E. Siggia [1982] "Universal Properties of the Transition from Quasi-periodicity to Chaos in Dissipative Systems", *Physica* (Utrecht) **6D**, 303-342.

[5] M. de Sousa Vieira, A. J. Lichtenberg and M.A. Lieberman [1991] "Nonlinear Dynamics of Self-synchronized Systems", *International Journal of Bifurcation and Chaos*, in press.

[6] L. M. Pecora and T. L. Carroll [1990] "Synchronization in Chaotic Systems", *Phys. Rev. Lett.* **64**, 821-824.

[7] J. Gullicksen, M. de Sousa Vieira, M. A. Lieberman, R. Sherman, A. J. Lichtenberg, J. Y. Huang, W. Wonchoba, M. Steinberg, and P. Khoury [1992] "Secure Communications by Synchronization to a Chaotic Signal", to appear in *Proceedings of the 1st Experimental Chaos Conference*, eds. M. F. Shlesinger, W. L. Ditto, L. Pecora and S. Vohra.

[8] W. Wonchoba, *in preparation.*

[9] See for example, A. J. Lichtenberg and M. A. Lieberman [1983] *Regular and Stochastic Motion*, Springer-Verlag.

[10] A. Wolf, J. B. Swift, H. L. Swinney and J. A. Vastano [1985] "Determining Lyapunov Exponents from a Time Series", *Physica* (Utrecht) **16D**, 285-317.

[11] H. G. Winful and L. Rahman [1990] "Synchronized Chaos and Spatiotemporal Chaos in Arrays of Coupled Lasers", *Phys. Rev. Lett.* **65**, 1575-1578.

[12] P. Grassberger and I. Procaccia [1983] "Measuring the Strangeness of Chaotic Attractors", *Physica D (Utretch)* **9**, 189-208.

[13] C. E. Shannon [1948] "The mathematical theory of communication", *Bell Syst. Tech. J.* **27**, 379-423; R. Shaw [1981] "Strange Attractors, Chaotic Behavior, and Information Flow", *Z. Naturforsch*, **36A**, 80-112; A. M. Fraser [1989] "Information and Entropy in Strange Attractors, *IEEE Trans. Inf. Theory* **35**, 245-262.

[14] Texas Instruments Incorporated [1981] *The TTL Data Book for Design Engineers*, Dallas, TX.

[15] National Semiconductor Corporation [1982] *Linear Databook*, Santa Clara, CA.

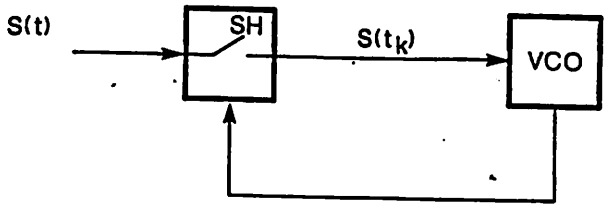

Fig. 1. Schematic representation of a single DPLL.

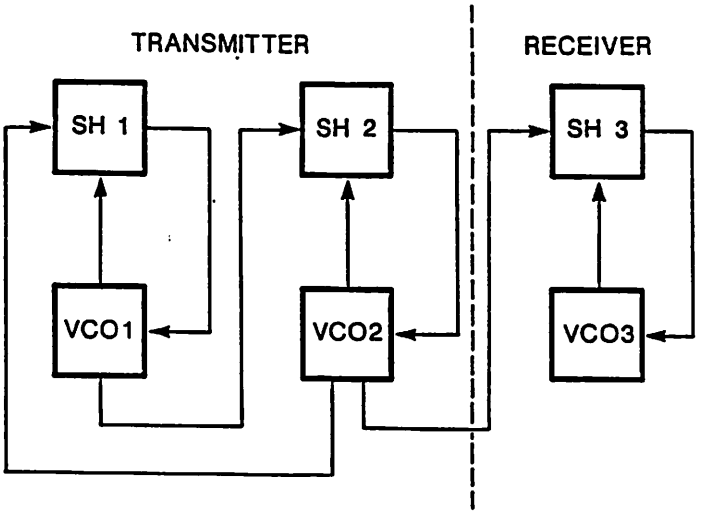

Fig. 2. Communication system consisting of three coupled DPLL's, with two self-synchronized loops as the transmitter.

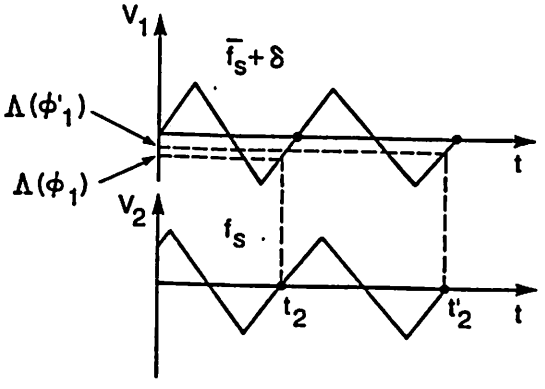

Fig. 3. Schematic representation of the dynamical evolution of the two coupled DPLL's after we perturb the frequency of the first loop in a system initially in the locked state.

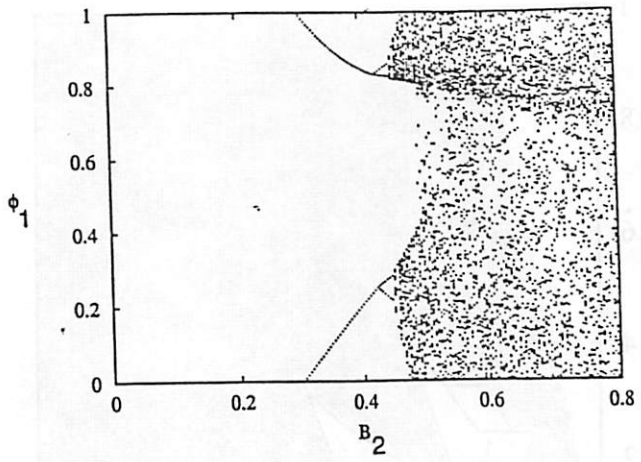

Fig. 4. Bifurcation diagram for $\phi_1(\phi_2 = 0)$ as as a function of B_2 for $B_1 = 0.2$ and $\overline{f}^o_1 = 1$.

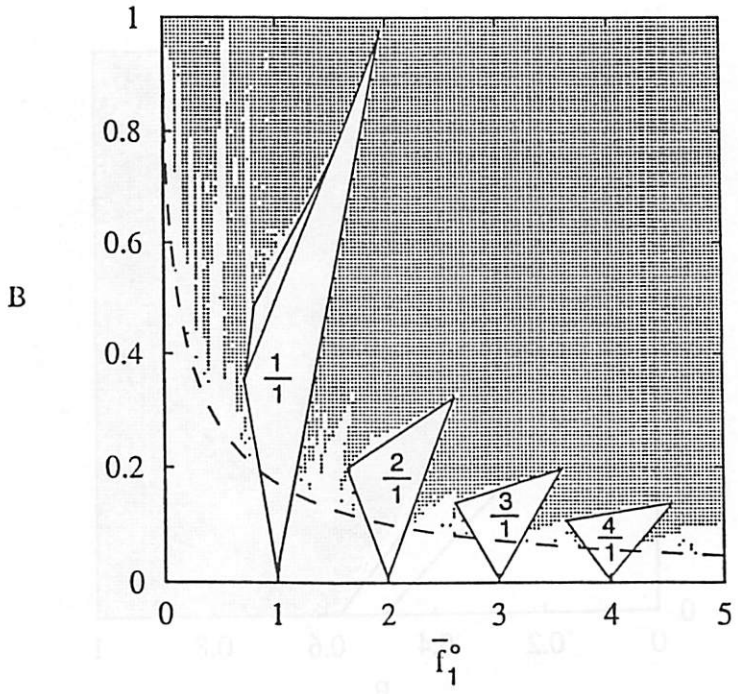

Fig. 5. Phase diagram of the map governed by Eq. (12) showing the chaotic region (dotted) and the periodic or quasiperiodic solutions (white). The border of invertibility is indicated by a dashed line and the largest "Arnold tongues" are labelled by the corresponding winding numbers. The 2/2 tongue is situated above the 1/1 tongue, and it is not labelled in the figure.

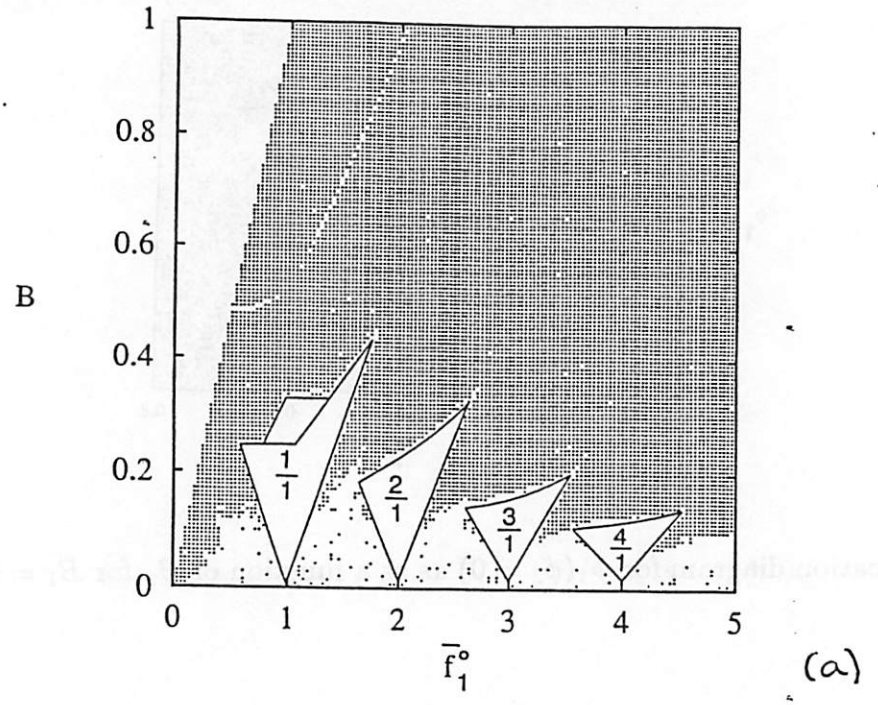

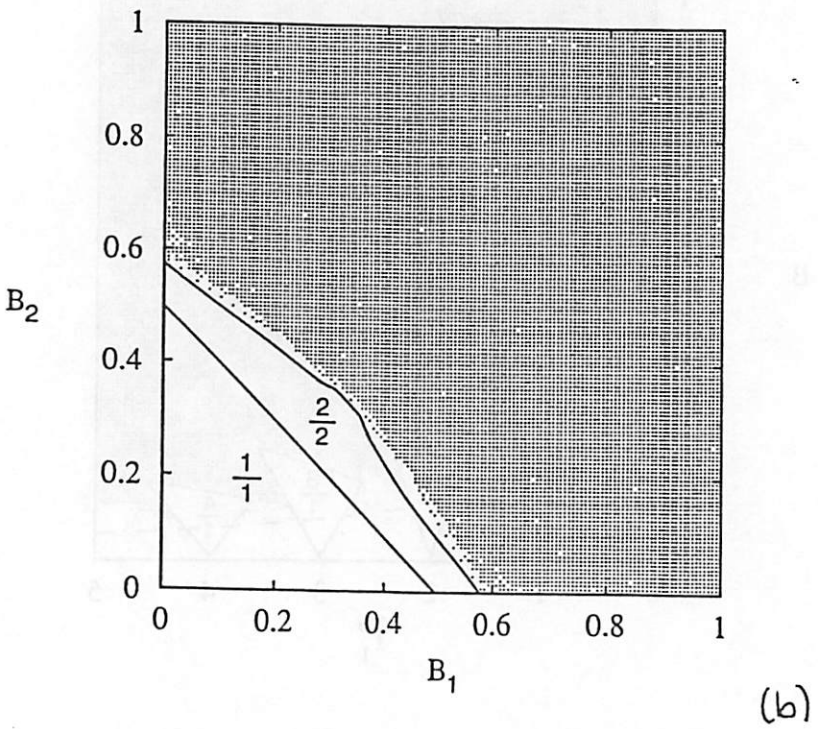

Fig. 6. Phase diagram for (a) $B \equiv B_1 = B_2$ vs. $\overline{f}_1^o$ and (b) B_2 vs. B_1 for $\overline{f}^o = 1$ showing the chaotic region (dotted). Some of the largest "Arnold tongues" are specified in the figure. The 2/2 tongue is situated above the 1/1 tongue, and it is not labelled in (a).

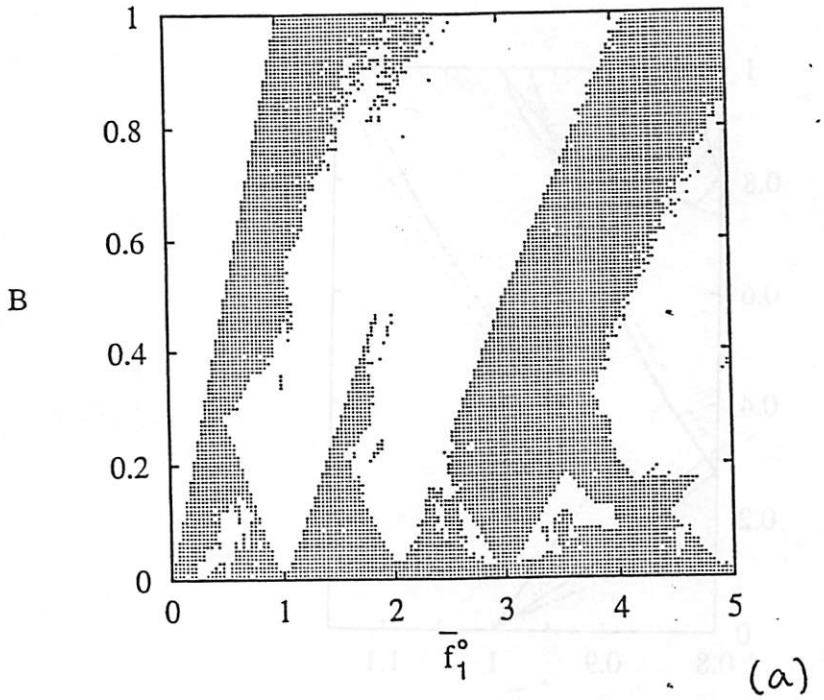

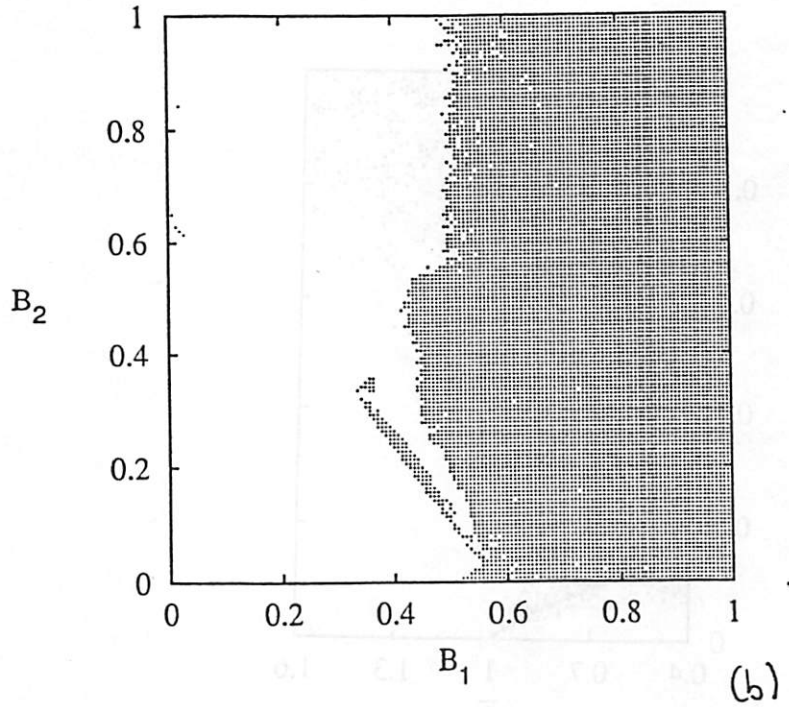

Fig. 7. Diagram showing the region of synchronization between loops 1 and 3 (white region) for (a) $B \equiv B_1 = B_2 = B_3$ vs. $\overline{f}_1^o$ and (b) B_1 vs. B_2 for $\overline{f}^o = 1$.

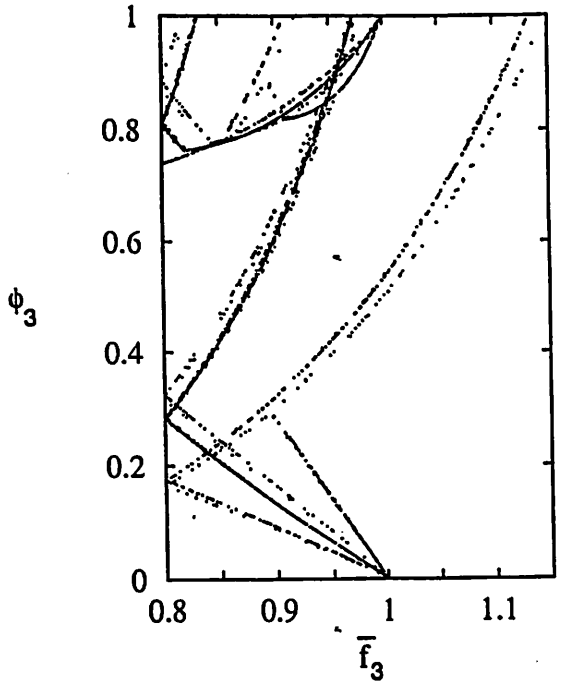

(a)

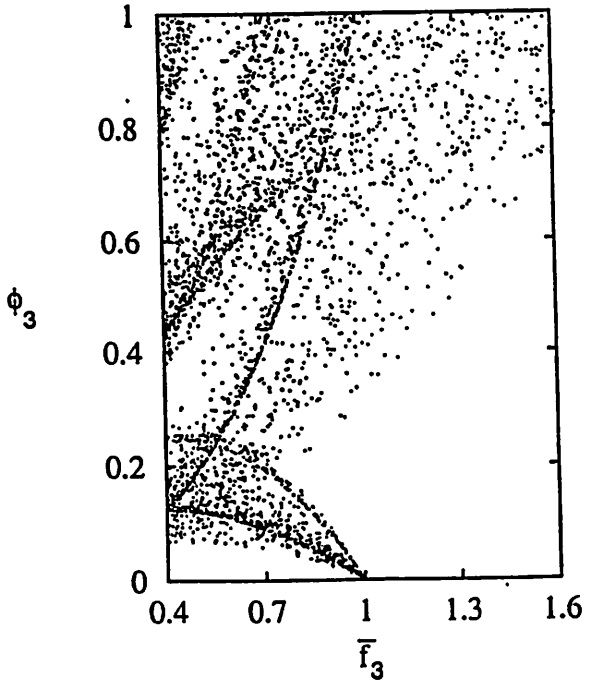

(b)

Fig. 8. Chaotic attractor ϕ_3 vs. $\overline{f}_3$ at $\phi_2 = 0$ for (a) $B_1 = B_3 = 0.2$, $B_2 = 0.6$ and (b) $B_1 = B_2 = B_3 = 0.6$ with $\overline{f}_1^o = \overline{f}_3^o = 1$. The plot of ϕ_1 vs. $\overline{f}_1$ for the first case is identical to ϕ_3 vs. $\overline{f}_3$ shown in 8a.

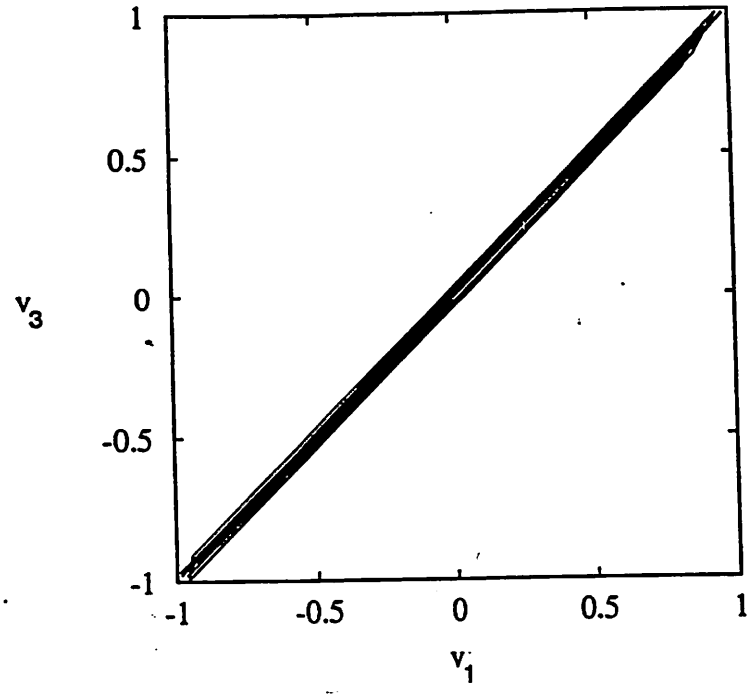

(a)

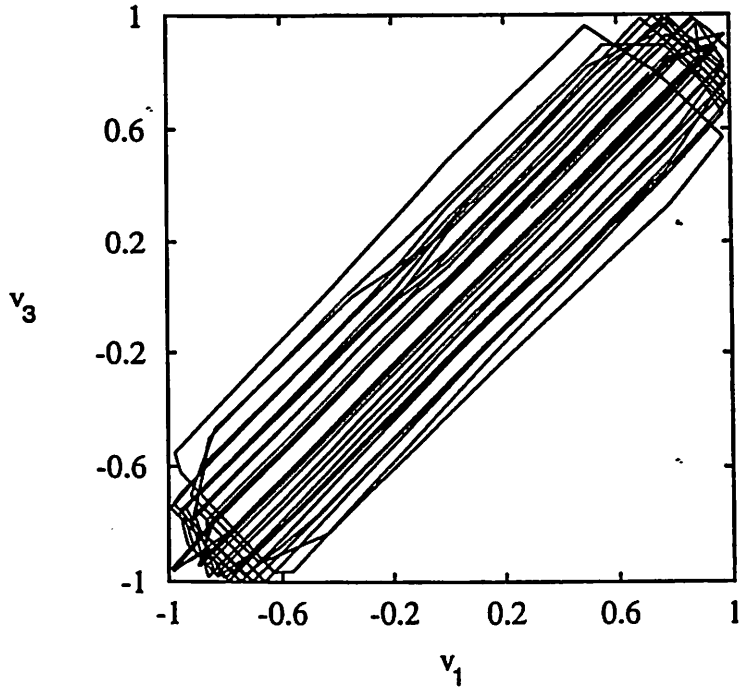

(b)

Fig. 9. v_3 vs. v_1 for (a) $B_1 = 0.2$, $B_2 = 0.6$, $B_3 = 0.21$ and $\overline{f}_1^o = \overline{f}_3^o = 1$, and (b) $B_1 = B_3 = 0.2$, $B_2 = 0.6$, $\overline{f}_1^o = 1$ and $\overline{f}_3^o = 1.01$.

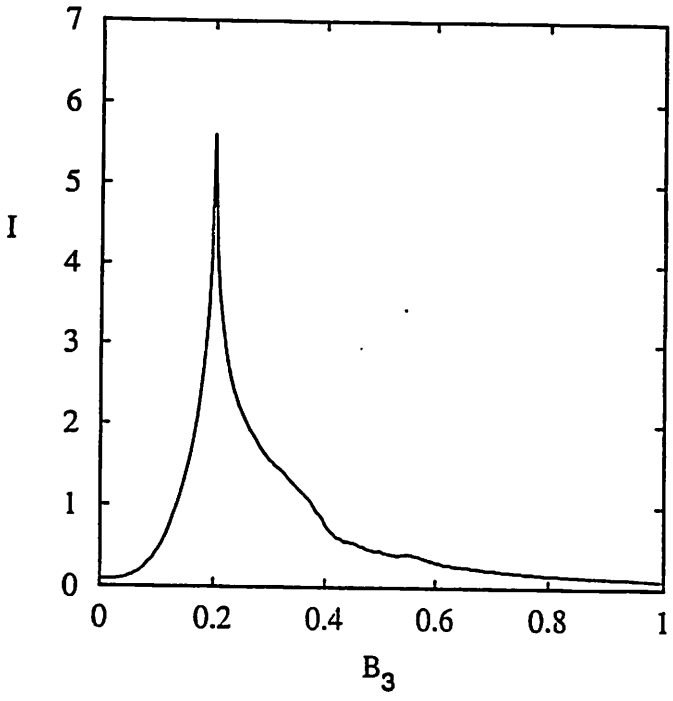

(a)

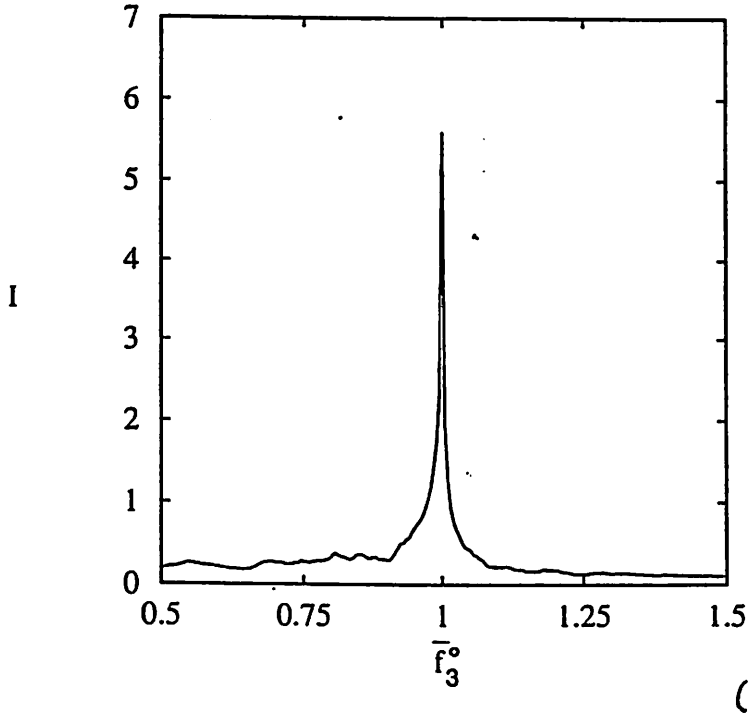

(b)

Fig. 10 Mutual information between loop 1 and loop 3 with $B_1 = 0.2$, $B_2 = 0.6$ and $\overline{f}_1^o = \overline{f}_3^o = 1$ for (a) I vs. B_3 and (b) I vs. $\overline{f}_3^o$.

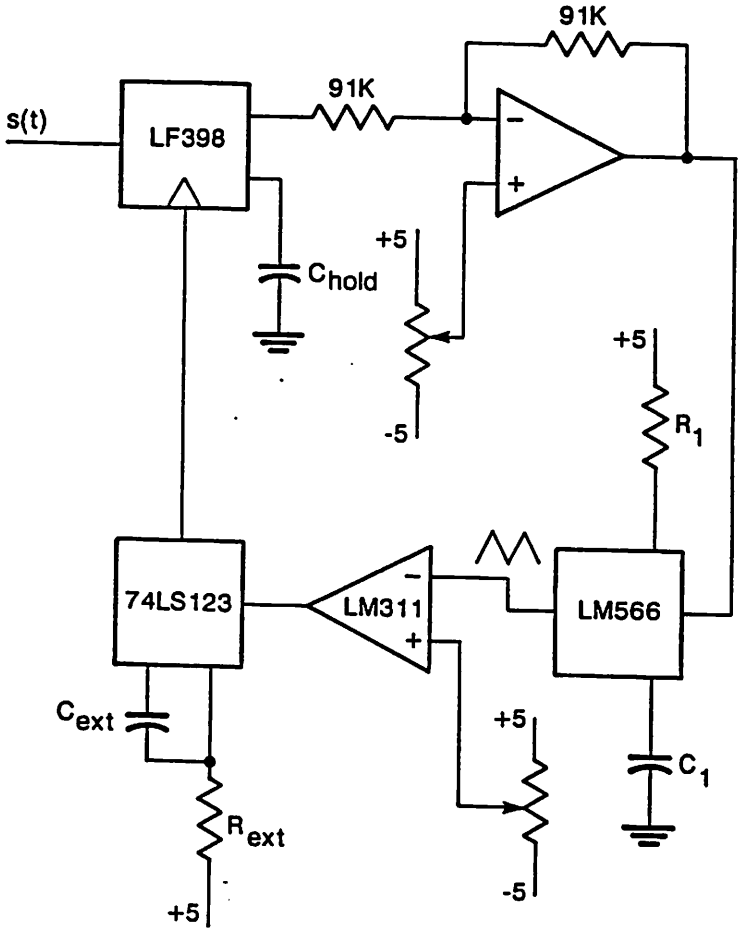

Fig. 11. Experimental implementation of a basic nonuniformily sampling first order DPLL.

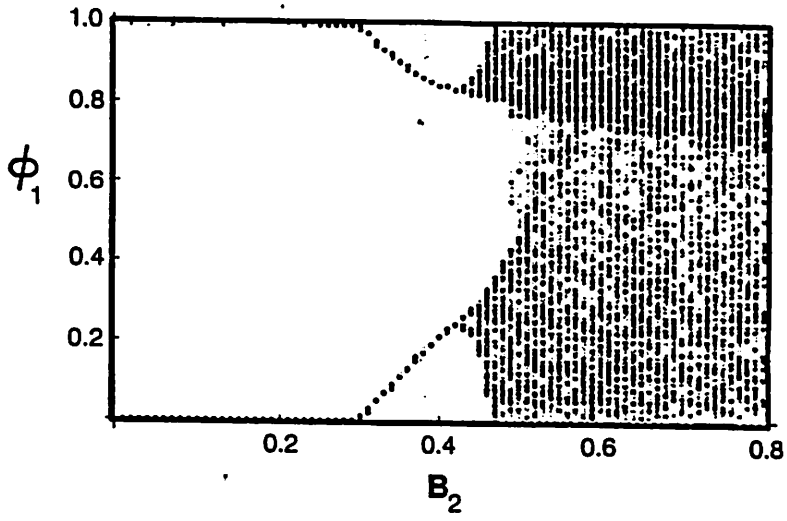

Fig. 12. Bifurcation diagram obtained experimentally for $\phi_1(\phi_2 = 0)$ vs. B_2, with the parameter values used numerically in Fig. 4.

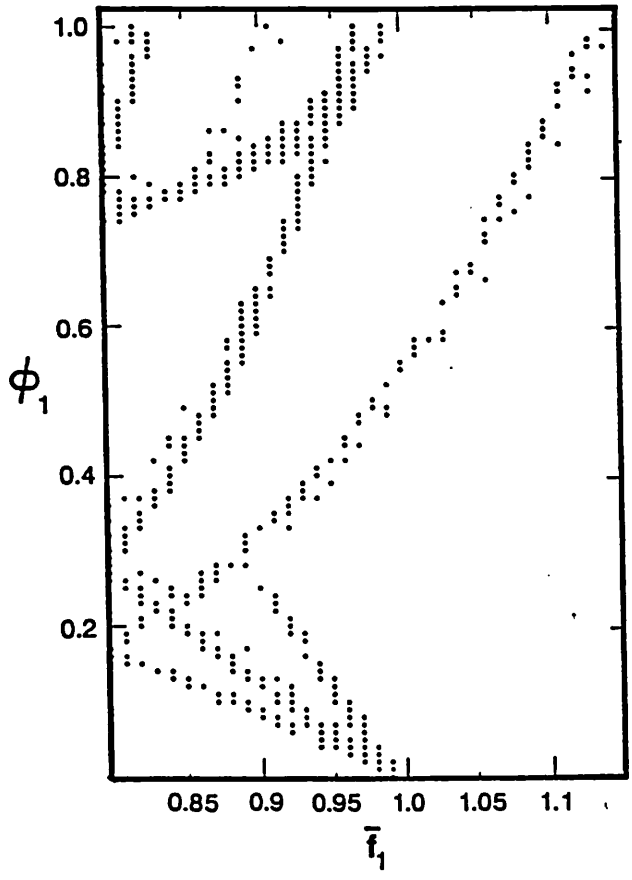

Fig. 13. Chaotic attractor obtained experimentally for ϕ_1 vs. $\bar{f}_1^o$ at $\phi_2 = 0$ with the same parameter values used numerically in Fig. 8a.

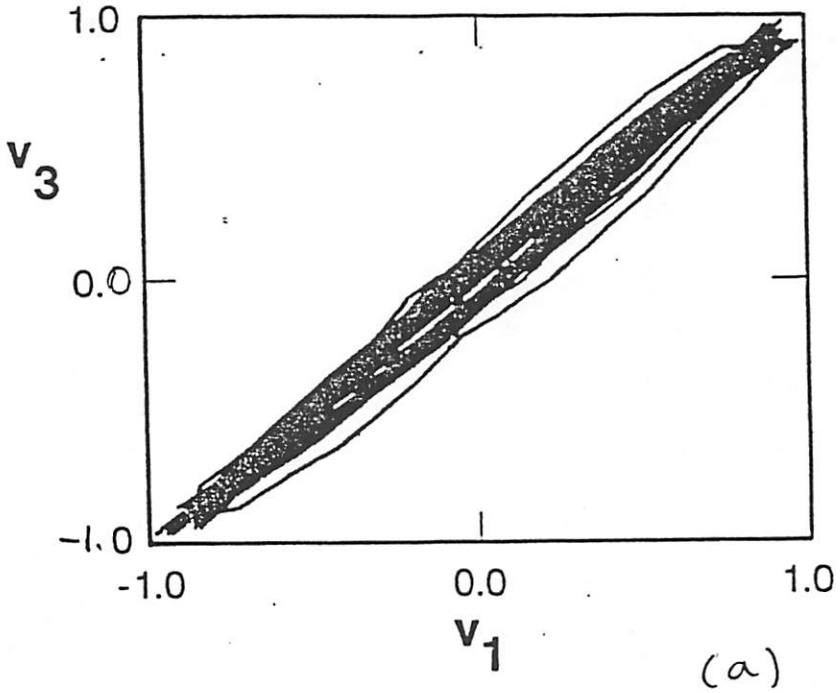

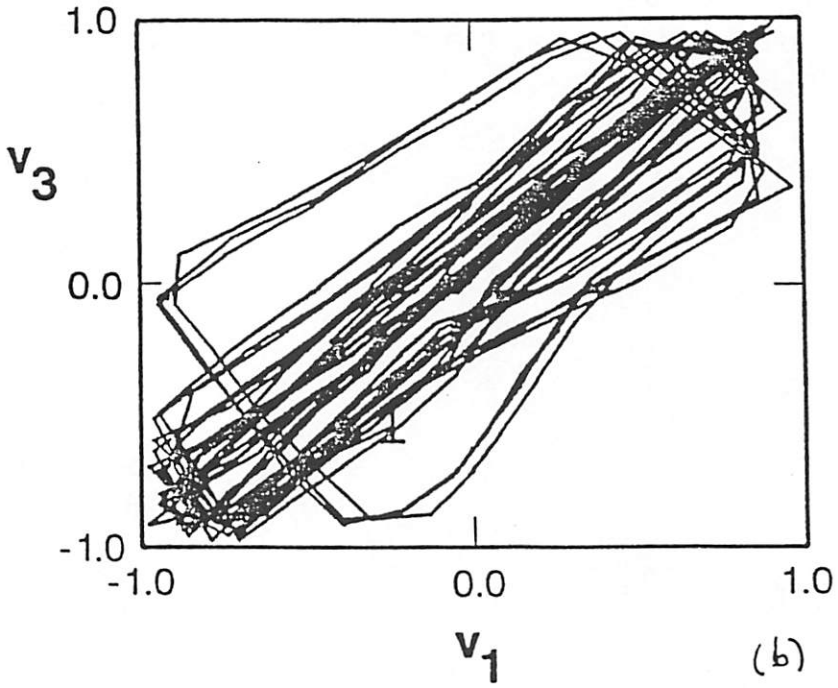

Fig. 14. (a) Chaotic synchronization obtained experimentally for the three loops systems for the parameter values $B_1 = 0.720$, $B_2 = 0.694$, $B_3 = 0.718$, $\overline{f}_1^o = 1.154$ and $\overline{f}_3^o = 1.152$. (b) Loss of synchronization observed when $\overline{f}_3^o$ is changed to $\overline{f}_3^o = 1.110$.